

# In situ FTIR spectroscopy of key intermediates in the first stages of ethylene polymerization on the Cr/SiO<sub>2</sub> Phillips catalyst: Solving the puzzle of the initiation mechanism?

Elena Groppo\*, Carlo Lamberti, Silvia Bordiga, Giuseppe Spoto, Adriano Zecchina\*

*Department of Inorganic, Physical and Materials Chemistry, and NIS Center of Excellence, University of Torino, via P. Giuria 7, I-10125 Torino, Italy*

Received 18 January 2006; revised 1 March 2006; accepted 10 March 2006

Available online 24 April 2006

## Abstract

We report here the first experimental observation, by means of in situ FTIR spectroscopy, of key intermediate species in the ethylene polymerization on the Cr(II)/SiO<sub>2</sub> Phillips catalyst. We demonstrate that by adopting suitable strategies, it is possible to shed light on one of the remaining questions concerning the system responsible for one-third of the worldwide polyethylene production: the puzzle of the initiation mechanism. “Anomalous” bands in the CH<sub>2</sub> stretching region are observed during the first steps of the polymerization reaction and assigned to small cycles on the Cr(II) sites, characterized by a structural strain decreasing with increasing ring dimension. These intermediate species are stable only in presence of a sufficiently high C<sub>2</sub>H<sub>4</sub> pressure and show a peculiar reactivity toward strong ligands, such as NO and O<sub>2</sub>. These results allow us to prove that the initiation mechanism follows a metallacycle route, similar to what occurs for several ethylene trimerization and tetramerization catalysts.

© 2006 Published by Elsevier Inc.

*Keywords:* Phillips catalyst; Metallacycle; Initiation mechanism; Chromium; Ethylene polymerization; In situ spectroscopy

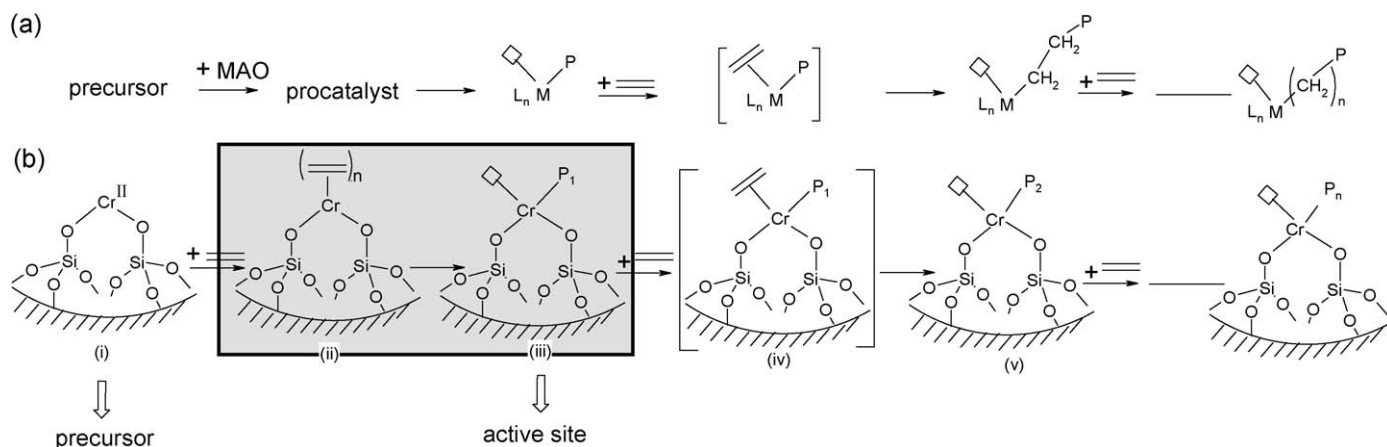
## 1. Introduction

The vast majority of the olefin polymerization catalysts used in the modern chemical industry are active only in presence of an activating agent (e.g., aluminum alkyl, methylalumoxane MAO). The ensemble constituted by the active precursor and the activating agents constitutes the so-called “procatalyst.” Whereas the structure of the precursor is generally known with good or sufficiently good precision, the structure of the active species formed through the intervention of the activating agents (procatalyst) is much less well characterized. In most cases, the hypotheses advanced on the reaction mechanism and the elementary reaction steps are based on the procatalyst and not on the active site structure. Here we consider “active sites” as only those species that are actually producing polymer chains by repeated insertion of monomer. Conversely,

species that can be transformed into active sites by some reaction, including initiation of a chain via reaction with C<sub>2</sub>H<sub>4</sub>, are merely “catalyst precursors” [1]. This is the case for heterogeneous catalysts for olefin polymerization (Ziegler–Natta or Union Carbide catalysts) as well as homogeneous ones (metallocene and Brookhart’s type catalysts), for which the active site is frequently prepared in situ from a transition metal compound not containing the active ligand (e.g., TiCl<sub>4</sub>, CrCp<sub>2</sub>) and an activator whose function is to introduce an alkyl group into the coordination sphere of the metal. A complete overview on the complexity of this problem, specifically concerning Cr-based systems, has been provided previously [1,2]. For these catalysts, a reaction mechanism in two steps is commonly accepted, as reported in Scheme 1a [3]. The preparation of the catalytic site requires the intervention of an activator (usually MAO), which introduces an alkyl group (P) in the coordination sphere of the metal site (M). The first step of the reaction is the coordination of a monomer molecule into a vacant position of M carrying the alkyl chain P via a d–π interaction; the second step is a migratory insertion reaction into the metal μ–alkyl bond that extends

\* Corresponding authors. Fax: +39 011 6707855.

*E-mail addresses:* [elena.groppo@unito.it](mailto:elena.groppo@unito.it) (E. Groppo), [adriano.zecchina@unito.it](mailto:adriano.zecchina@unito.it) (A. Zecchina).



Scheme 1. (a) Scheme of the initiation mechanism in the ethylene polymerization for a Ziegler–Natta type catalyst, according to the Cossee-type mechanism [3]. The active site, obtained by a precursor with the intervention of an activator (usually MAO), is a transition metal M characterized by the presence of an alkyl chain P and an available coordination site. (b) Scheme of the initiation mechanism in the ethylene polymerization for the Phillips-type catalyst, according to a Ziegler–Natta like behavior. The precursor of the active site is a Cr(II) species. The active site is generated by ethylene itself. The nature of the intermediate species inside the “black box,” which can be considered as the “precursor pool,” is unknown.

the growing alkyl chain P by one monomer unit, thereby regenerating the vacant coordination site at the metal center.

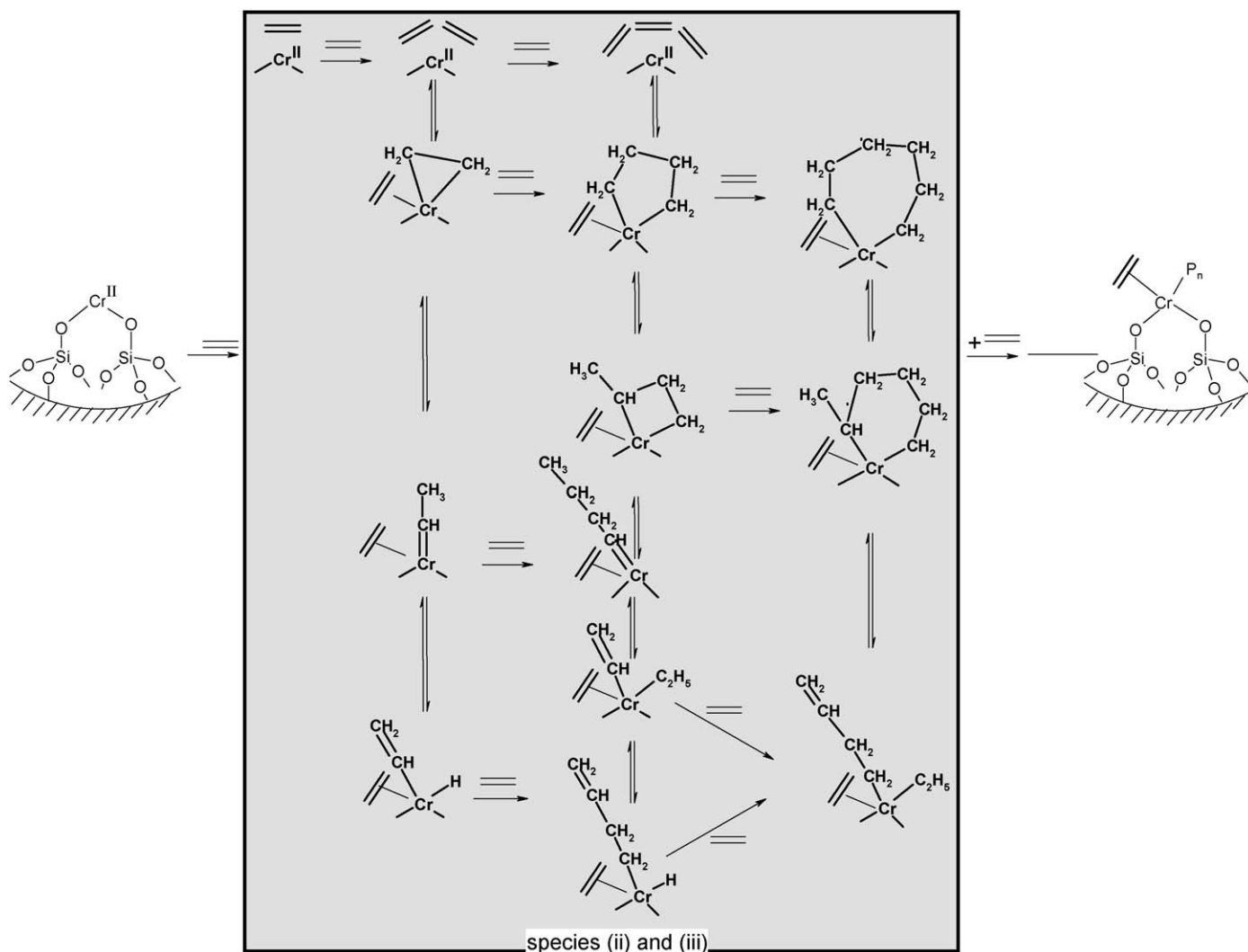
In contrast to the previously cited cases, the Cr/SiO<sub>2</sub> Phillips catalyst [4] is able to polymerize ethylene without the intervention of an activator, a property that simplifies the catalyst preparation and production processes as well as, in principle, the mechanistic investigations. The absence of an activating agent makes the Phillips catalyst peculiar and somewhat mysterious but also one of the rare catalytic systems in which the investigation of the reaction mechanism can directly involve the real active sites (or their precursors), not only the procatalyst. For this reason, the Phillips catalyst is taken here as an unique and challenging example to verify the possibilities and problems that can be encountered in an investigation designed to experimentally detect the intermediate species formed during the ethylene initiation and polymerization reaction, with the aim of identifying its initiating mechanism.

This is the reason why in recent years much work has been done on clarifying the structure of the precursors of the Cr active sites [anchored Cr(II) species] for both the industrial [Cr(VI)/SiO<sub>2</sub>] and CO-reduced [Cr(II)/SiO<sub>2</sub>] systems, obtained simply by reduction of the surface chromate precursors with CO at 623 K [5]. Several spectroscopic techniques have been adopted to highlight the coordination environment of the surface Cr species. From UV–vis DRS [5–9], FTIR spectroscopy of adsorbed probe molecules (CO, NO, CO<sub>2</sub>, N<sub>2</sub>O, pyridine, and, more recently, H<sub>2</sub> and N<sub>2</sub>) [5,10–24], Raman spectroscopy [5,9,25,26], resonant or preresonant Raman spectroscopy [27, 28], XAS [5,8,29], and XPS [5,30,31], an extremely complex and heterogeneous scenario has emerged, reflecting the high heterogeneity of the silica support [5]. Recently, we demonstrated a precise relationship between the structure of the precursors of the Cr active sites, the polymerization activity, and the properties of the resulting polymers [32]. In particular, we showed that the origin of the broad molecular weight (MW) distribution characterizing the Phillips polyethylene (PE) is strongly related to the presence of a distribution of Cr sites,

all active in ethylene polymerization but characterized by different turnover frequencies (TOFs) of the C<sub>2</sub>H<sub>4</sub> insertion reaction [32].

Despite significant recent progress in the investigation of the structural features of the Phillips catalyst, a definite explanation of the polymerization mechanism has not yet been achieved. By analogy with the Cossee-type mechanism advanced for the Ziegler–Natta and metallocene catalysts (see Scheme 1a), the general polymerization mechanism on the Phillips catalyst should be expressed as in Scheme 1b. In both schemes, a precursor species of the active site (procatalyst) is transformed into the real active site: in the classical Ziegler–Natta or metallocene catalysts, as already discussed, this transformation step requires the intervention of an activating agent. Conversely, in the Phillips catalyst, formation of the active site exploits an unknown promotion from ethylene itself, as represented in Scheme 1b. In this scheme, the anchored Cr(II) species [structure (i)] is the precursor of the active site and Cr–P<sub>1</sub> [structure (iii)] is the active site, with P<sub>1</sub> a hydrocarbon chain of unknown structure formed from the initially coordinated ethylene [structure (ii)]. Note that recently the formation of Cr(II)···(C<sub>2</sub>H<sub>4</sub>)<sub>n</sub> π-bonded complexes [structure (ii)] was revealed by FTIR spectroscopy [24]. After the creation of P<sub>1</sub> groups, the mechanism proceeds via the usual Cossee-type insertion of an ethylene molecule with formation of the intermediate species represented in square brackets [structure (iv)]. The nature of P<sub>1</sub> intermediates remains an open question. Several structures have been proposed in the literature, and the “black box” of Scheme 1b has been filled with different structures, as reported in Scheme 2. The numerous species present in the “black box” form a “precursor pool” in which some species could even be in mutual equilibrium.

The hypothesized species contained in the black box of Schemes 1b and 2 have not yet been identified, mainly for two reasons: (1) Only a fraction of the Cr sites are really active in the polymerization under the usually adopted experimental conditions [5,33], so that almost all the characterization tech-



Scheme 2. The “precursor pool” proposed in literature for the Cr(II)/SiO<sub>2</sub> catalyst. The “black box” represented in Scheme 1b contains here all the proposed P<sub>1</sub> structures. In the horizontal direction the evolution of the initial species upon addition of one ethylene molecule is represented. In vertical direction, all the possible isomeric structures characterized by an average C<sub>2</sub>H<sub>4</sub>/Cr ratio equal to 1, 2 and 3 are reported. See Ref. [5] for a more detailed description of the proposed mechanisms. Note that the structure of the Cr(II) sites is oversimplified, being not represented the weaker ligands present into their coordination sphere.

niques give information mainly on the inactive Cr sites, and (2) the active sites are characterized by a very high polymerization rate (high TOF) [5,33]. It is thus clear that any experimental effort devoted to detection of the precursor species must be designed to solve these two problems. From a general standpoint, the possibility of detecting a precursor species by spectroscopic methods is related to (a) the lifetime of the intermediate, because only those species with lifetimes greater than the time needed to perform the experiment can be detected [34], and (b) the sensitivity of the experimental method. Progress in direction (a) can be achieved by improving the time response of the instrument, finding a way to slow down the reaction speed, or both. Concerning direction (b), it must be emphasized that among all of the spectroscopic techniques, FTIR spectroscopy is the most versatile and surely has been the most widely used in attempts to identify the precursors of a reaction, being able to directly discern between the vibrational manifestations of different species even under operando conditions [5,23,34]. With respect to other techniques, FTIR spectroscopy can also be ap-

plied to diluted and thick samples still containing a sufficient number of active sites. This implies that it is useful in detecting species present in low concentration. For these reasons, FTIR spectroscopy, in both the conventional and temperature-resolved versions, has been chosen here to face the challenge of identifying the initiation mechanism on the Phillips catalyst, that is, to elucidate the nature of the intermediate species P<sub>1</sub> (see Schemes 1b and 2).

## 2. Experimental

The Cr(II)/SiO<sub>2</sub> samples (1 wt% Cr) were prepared by impregnating silica-aerogel monoliths with a solution of CrO<sub>3</sub> in CH<sub>3</sub>CN. The aerogel monoliths, kindly supplied by Novara Technology [35], had a surface area of about 700 m<sup>2</sup> g<sup>-1</sup>. After the impregnation step, the aerogel fragments were dried at room temperature, reduced in powder, and pressed into thick (~0.5 mm) pellets. Even after grinding, the silica-aerogel guarantees an almost complete transparency of the sample in the IR

region in the 4500–1800  $\text{cm}^{-1}$  range, because of the absence of scattering [24,27]. The pellets were then transferred into an IR cell designed to allow thermal treatment of the sample in the 1000–77 K range, either under vacuum or in the presence of a desired equilibrium pressure of gases. The samples were subjected to the following treatments: activation at 923 K; calcination in  $\text{O}_2$  at the same temperature for 1 h; reduction in CO at 623 K, followed by CO removal at the same temperature; and cooling to room temperature. The FTIR spectra were collected on a Bruker IFS-66 spectrophotometer at 2  $\text{cm}^{-1}$  resolution.

### 3. Results and discussion

#### 3.1. Previous attempts and new strategies

In the past, several attempts have been made to identify the species formed in the initial steps of the ethylene polymerization reaction on the Cr/SiO<sub>2</sub> system by means of FTIR spectroscopy [5,15,23,36,37]. It is well known that by carrying out the reaction on a CO-reduced Cr(II)/SiO<sub>2</sub> system at room temperature, only the vibrational manifestations of the growing polymeric chains can be detected, at 2920 and 2851  $\text{cm}^{-1}$  [13,15,17,21].

Conversely, several authors have reported the appearance in the first stages of the reaction of few bands assigned to Cr(II)··C<sub>2</sub>H<sub>4</sub> complexes by decreasing the ethylene polymerization rate; however, these bands were characterized by a transient character [15,36,37]. More recently, some of us [23] attempted to address the problem by lowering the rate of the polymerization reaction. This goal was achieved by working at low temperature and in the presence of CO acting as a poison in the propagation step. In the 100–130 K range, ethylene formed mixed Cr(II)··(CO)(C<sub>2</sub>H<sub>4</sub>) complexes [23], whereas with increasing temperature, C<sub>2</sub>H<sub>4</sub> gradually displaced CO, and polymerization began at a much slower rate than on the samples without CO. The low reaction speed allowed the observation of new, weak features not detected in the usual polymerization experiments [23]. In particular, at the lowest reaction times, besides the usual 2920 and 2851  $\text{cm}^{-1}$  peaks characteristic of long polymeric chains [5], two weak shoulders at 2931 and 2860  $\text{cm}^{-1}$  were observed, which were attributed to the  $\nu(\text{CH}_2)$  modes of short polymeric chains. These preliminary experiments provide strong evidence that a combination of low temperature, low monomer pressure, selective poisoning of the propagation reaction, and short observation times could provide insight into the species characterizing the “initiation pool” (black box in Schemes 1b and 2).

Increased sensitivity can be achieved by acting simultaneously on three factors: (1) increasing the number of active sites probed by the IR beam, (2) using thick pellets with low scattering properties, and (3) adopting a support with a very high surface area. Success in this direction has recently been achieved using a SiO<sub>2</sub>-aerogel as a support for the Cr(II) species [5,24,27]. In fact, the high transparency of this support in the IR region and the peculiar scattering properties allowed us to work in transmission mode with very thick pellets without loss of transparency. This, together with the fact that the SiO<sub>2</sub>-aerogel has

a greater surface area than the common SiO<sub>2</sub>-aerosil, suggests that an order-of-magnitude increase in the number of Cr sites probed by the IR beam, and thus in the probability to detect very weak bands, such as those expected from the few species present in the first steps of the reaction, can be obtained. The key role of SiO<sub>2</sub>-aerogel in detecting the Cr(II)··(C<sub>2</sub>H<sub>4</sub>)<sub>n</sub>  $\pi$ -bonded complexes [24], the very first precursors of the reaction, was recently demonstrated; see structure (ii) in Scheme 1b, as mentioned earlier.

Finally, we have demonstrated that different families of Cr(II) sites characterized by a wide distribution of catalytic activity are present on the amorphous silica surface, and that suitable annealing procedures provide reliable means of tuning the relative populations of the different families of Cr(II) sites [32]. Knowledge of the relationship between the active site structure and the catalytic activity [32] suggests that the sites with slower C<sub>2</sub>H<sub>4</sub> insertion (Cr<sub>A</sub><sup>II</sup>, as described previously [5,11,13,15,21,23]) should be the best suited for spectroscopic investigation of the species present in the “black box.” For this reason, the FTIR experiments were conducted on a sample characterized by both a high number of Cr sites and also a maximized fraction of “slow” sites (Cr<sub>A</sub><sup>II</sup>) with respect to the “fast” sites (Cr<sub>B</sub><sup>II</sup>). Details on the experimental conditions that influence the Cr population have been reported previously [32].

#### 3.2. Observation of “anomalous” bands

On the basis of the foregoing considerations, we performed in situ temperature-resolved FTIR experiments at low C<sub>2</sub>H<sub>4</sub> pressure on a thick Cr(II)/SiO<sub>2</sub>-aerogel sample characterized by a high Cr<sub>A</sub><sup>II</sup>/Cr<sub>B</sub><sup>II</sup> ratio at low temperature. The number of dosed ethylene molecules was of the same order of magnitude of the total number of chromium sites present in the sample. The results are shown in Fig. 1a, which reports a sequence of spectra collected at increasing temperature (starting from 100 K and extending to room temperature) and increasing polymerization times (i.e., time- and temperature-resolved spectra). The thickness of the silica pellet and the subsequent high intensity of the SiO<sub>2</sub> bulk modes at frequencies below 2000  $\text{cm}^{-1}$  allowed observation of the CH<sub>2</sub> stretching region only. At  $T \sim 100$  K, the Cr(II)··(C<sub>2</sub>H<sub>4</sub>)<sub>n</sub>  $\pi$ -bonded complexes were the only species formed, as demonstrated by the presence of narrow bands at 3004, 3084, and 3104  $\text{cm}^{-1}$ , only the first of which is shown in Fig. 1a for clarity [23,24]. These bands were accompanied by a weak component at about 2975  $\text{cm}^{-1}$  (● in Fig. 1a), due to the C<sub>2</sub>H<sub>4</sub> molecules in interaction with the silanol groups (as indicated by the permanent band at about 3650  $\text{cm}^{-1}$ , due to perturbation of the Si–OH groups; spectral region not shown). Increasing the temperature initiates the polymerization, as evidenced by the growth of the CH<sub>2</sub> stretching bands at 2925 and 2855  $\text{cm}^{-1}$  associated with the growing polymeric chains (☆ in Fig. 1a). However, in the first stages of the polymerization reaction, two new bands at 2931 and 2861  $\text{cm}^{-1}$  were clearly evident, accompanied by a very weak component at about 2965  $\text{cm}^{-1}$  (★ in Fig. 1a). In what follows we refer to these bands as “anomalous,” because they are associated with species very different from the polymer chains and can be ob-



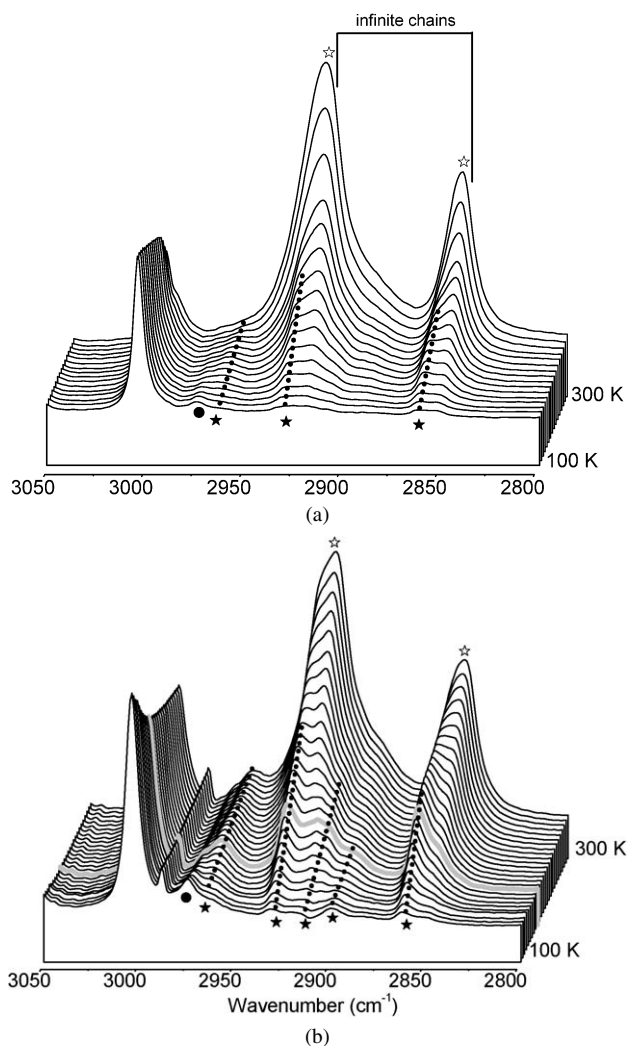


Fig. 1. Temperature-resolved ethylene polymerization on Cr(II)/SiO<sub>2</sub>, in the 100–300 K range, in absence (part a) and in presence of a CO poison (part b). Only the C–H stretching region is shown. The first curve is dominated by the ethylene  $\pi$ -complexes at the highest ethylene pressure (peak at 3004 cm<sup>-1</sup>) and by the almost total absence of polymerization products, which progressively appear in the successive spectra (☆). For comparison, the frequency position of infinite polymeric chains is also shown (black lines in part a). The weak component at 2975 cm<sup>-1</sup> (●) is due to the residual C<sub>2</sub>H<sub>4</sub> molecules still in interaction with the silanol groups. The anomalous bands present in the first stages of the polymerization are evidenced by a ★ and their evolution by dotted lines. The gray spectrum will be the starting point in the successive figures.

observed only during the initial phases of the reaction. The novelty of these results with respect to those reported previously [23] is that, due to the novel experimental conditions, these bands are more intense and better resolved. Note also that the two bands associated with the growing polymeric chains (☆ in Fig. 1a) are at frequencies  $\sim 6$  cm<sup>-1</sup> higher than those characterizing the crystalline polyethylene (see the black lines in Fig. 1a). This shift is easily explainable by considering that the first short polymeric chains are characterized by a higher conformational disorder than the infinite polymeric chains [32,38–44]. In this sense the spectra shown in Fig. 1a are “anomalous” with respect to all of the components, confirming that we are seeing

the spectroscopic manifestations of species formed during the very early stages.

On the basis of this observation and the earlier discussion on the interfering effect of CO in the propagation reaction, we performed experiments in the presence of CO with the aim of lowering the propagation rate and hence increasing the concentration of initial species and consequently of anomalous bands. The results, shown in Fig. 1b, are analogous to those for the experiment reported in Fig. 1a, but performed in the presence of CO poison (10 Torr of C<sub>2</sub>H<sub>4</sub> in a CO equilibrium pressure of 0.5 Torr). The complex bands shown in Fig. 1b are very similar to those already observed in the absence of CO (see Fig. 1a). However, the anomalous bands at 2931, 2861, and 2965 cm<sup>-1</sup> are now much more intense and better resolved, and in addition two bands at 2915 and 2893 cm<sup>-1</sup> are clearly evident in the very initial steps. This important result demonstrates not only that our hypothesis is correct, but also that we can now intervene in a rational way in the reaction mechanism. By allowing the reaction to proceed simply by increasing temperature, the anomalous bands are slowly overshadowed by the standard CH<sub>2</sub> stretching bands of the growing polymeric chains (☆ in Fig. 1b). Conversely, if the reaction is suddenly stopped at low temperature by evacuating the IR cell, then the anomalous bands rapidly disappear with reduced ethylene equilibrium pressure, and only weak bands corresponding to the CH<sub>2</sub> stretching modes of the  $-(\text{CH}_2-\text{CH}_2)_n-$  groups of polymer chains remain (see Fig. 2, from gray to black spectrum). This phenomenon is reproducible, and a new admission of ethylene (under the same experimental conditions—i.e., low temperature in the presence of CO) once again allows detection of the anomalous bands (spectra not shown for brevity). Due to the small number of dosed ethylene molecules, the  $n$  value of the chains thus formed cannot exceed 10–15. Because hydrocarbon chains of the type R-(CH<sub>2</sub>-CH<sub>2</sub>) <sub>$n$</sub> -R terminating with R = CH<sub>3</sub> should demonstrate distinct absorption due to  $\nu_a(\text{CH}_3)$  [5], the irreversible species can be inferred to have a cyclic structure. Note that the relative C<sub>2</sub>H<sub>4</sub>/CO ratio plays an important role in determining the polymerization rate and thus in the clear observation of the intermediate species. A too-high C<sub>2</sub>H<sub>4</sub>/CO ratio does not allow observation of the intermediate species, because the polymerization reaction is too rapid; conversely, a too-low ratio does not allow initiation of the polymerization reaction.

It is worth mentioning that the anomalous components observed in Fig. 1b are very similar to those observed in the initial steps when polymerization was conducted at low temperature on a Cr/SiO<sub>2</sub>-aerogel sample in the absence of CO poison (see Fig. 1a). These observations exclude the possibility that the origin of the anomalous bands is in some way linked to the presence of CO. In fact, because CO does not interfere with observation of the anomalous bands, it can be safely inferred that it acts exclusively on the propagation mechanism, being a competitor of ethylene in structure (iv) of Scheme 1b. Conversely, CO does not modify the nature of the species contained in the black box in Scheme 1b characterized by the presence of a hydrocarbon chain. Thus, it is clear that we are detecting some of the intermediate species of the black box, which are stable

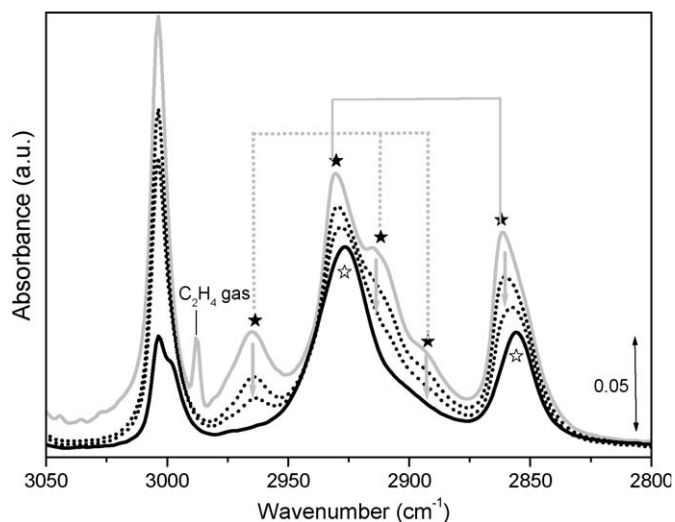


Fig. 2. Evolution of the anomalous bands upon outgassing, from the grey spectrum (obtained in the same conditions of that reported in Fig. 1b) to the black one through the dotted ones. The grey arrows show the decrease of the anomalous bands. Symbols as in Fig. 1. A tentative coupling of the bands in terms of stretching modes belonging to the same species is reported with dotted and full gray lines.

only in the presence of sufficiently high  $C_2H_4$  pressure and are rapidly consumed by the propagation reaction. The ability to interfere with the stability of these species allows us to state some preliminary hypotheses on the initiation mechanism.

### 3.3. Interpretation of the anomalous bands and hypotheses on the initiation mechanism

The species present in the black box of Scheme 2 can be divided in two main groups: those with a metallacycle structure (second row) and those carrying a  $CH_3$  group (bottom part). The metallacycle mechanism involves the coordination of one, two or three  $C_2H_4$  molecules to the Cr(II) site, followed by the formation of chromacyclopropane or chromacyclopentane species, which then can grow in dimension on  $C_2H_4$  insertion. Conversely, the methyl group is formed via H transfer from ethylene to the Cr site; for this region, it is difficult to imagine that the species belonging to the second group can be reversible to outgassing at room temperature. These considerations lead us to strongly support the hypothesis that the anomalous bands are associated with small metallacycles and that the initiation mechanism follows a metallacycle route, as hypothesized previously [5,13,21,23].

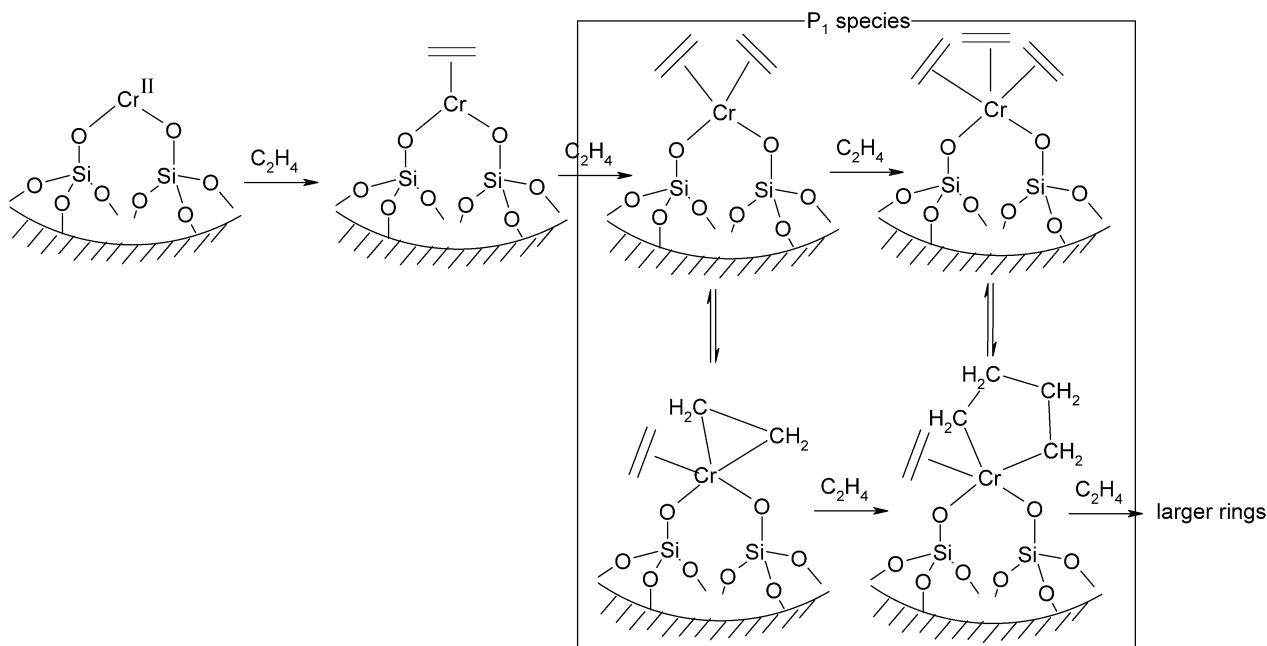
In our opinion, the aforementioned data offer the first spectroscopic characterization of such metallacycle intermediates on the basis of two important considerations. First, the anomalous bands are characterized by stretching frequencies higher than those of  $CH_2$  groups belonging to long linear alkane chains [ $\nu(CH_2)$  at 2920 and 2850  $cm^{-1}$  for crystalline PE [42]]. It is known that the values of the  $\nu(CH_2)$  stretching bands are sensitive indicators of the extent of lateral interaction between  $n$ -alkyl chains, and in particular that a shift toward higher wave numbers indicates increased conformational disorder. However, a shift of only about  $+6\text{ cm}^{-1}$  with respect to the  $\nu(CH_2)$  modes

of long polyethylene chains has been reported for short alkyl chains [32,38–44]. This explains the 2925 and 2855  $cm^{-1}$  values characterizing the growing polymeric chains ( $\star$  in Fig. 1a). However, these values are definitely lower than those characterizing the anomalous bands, especially for the bands at 2965, 2915, and 2893  $cm^{-1}$  (see the gray dotted lines in Fig. 2). These high-frequency values may be explained in terms of the  $\nu(CH_2)$  modes of little metallacycles characterized by a strong geometric strain. For comparison, consider that the  $\nu_a(CH_2)$  and  $\nu_s(CH_2)$  stretching frequencies of cyclopropane, cyclobutane, and cyclohexane shift progressively from 3103–3025  $cm^{-1}$  to 2987–2887  $cm^{-1}$  and then to 2933–2863  $cm^{-1}$ .

Second, the transient character of the anomalous bands on outgassing (see gray arrows in Fig. 2) suggests that they belong to intermediate species that are stable only in the presence of sufficiently high  $C_2H_4$  pressure. In other words, steps (ii)  $\rightarrow$  (iii) in Scheme 1b should be better represented as an equilibrium that shifts completely to the left side of the reaction with decreasing  $C_2H_4$  pressure. This behavior can be explained by considering that as the polymerization proceeds, the concentration of the strained metallacycle species decreases. We thus observe a constant and gradual shift of the  $\nu(CH_2)$  bands toward lower frequencies, resulting in disappearance of the anomalous bands and growth of the standard  $CH_2$  stretching bands characterizing polyethylene chains. Note that evidence of the reversibility of metallacyclopentane species in the case of titanacyclopentanes has been provided by Bre et al. [45].

The possible existence of metallacyclic reaction intermediates has been known since the 1970s, when McDermott et al. [46] demonstrated the existence of Pt(II) metallacycles. Support for the metallacycle mechanism involving Cr sites come from the publication of crystal structures of 5- and 7-membered Cr metallacycle species [47,48]. Several authors have also provided evidence of the validity of such a metallacycle mechanism for  $C_2H_4$  trimerization and tetramerization reactions occurring on Cr-based homogeneous catalysts [47,49–53], supported by computational studies [54]. Very recently, experimental evidence (from gas chromatography and mass spectrometry analysis) for large-ring metallacycle intermediates in polyethylene chain growth using homogeneous Cr catalyst has been provided [55]. However, to date no spectroscopic evidence of the existence of Cr-metallacycle intermediates in  $C_2H_4$  polymerization reaction on the heterogeneous Phillips-type catalyst has been presented, and only hypotheses based on the absence of vibrational manifestations belonging to terminal groups have been made. The reason for this is mainly related to the very short lifetimes of these species, as discussed in Section 1.

Based on the foregoing considerations, we rewrote Scheme 1b by representing the  $P_1$  species as metallacycle species (see Scheme 3). The starting point could be a  $Cr \cdots (C_2H_4)_n$  ( $n = 1, 2, 3$ ) species that then evolves into a Cr-cyclopropane or Cr-cyclopentane structure. These metallacycle intermediates represent the actual catalytic sites. However, it is worth mentioning that even if the initiation mechanism now seems well defined, no definite conclusions about the successive evolution of the metallacycle species can be drawn. In fact, the results here refer to the insertion of a very limited number of eth-



Scheme 3. Schematic representation of the metallacycle mechanism hypothesized on the basis of the observation of “anomalous” bands in the FTIR spectra of ethylene polymerization on the Cr(II)/SiO<sub>2</sub> system. A specific initiation mechanism has been identified inside the “black box” reported in Scheme 2.

ylene molecules per Cr site, and nothing can be stated about the successive propagation step leading to formation of the actual polymer chains. In particular, the propagation reaction can follow at least three different paths: (a) progressive insertion of monomer molecules inside the metallacycles, which then grow in dimension; (b)  $\beta$ -hydride transfer from the metallacycle to a coordinated ethylene (or to Cr, with subsequent ethylene insertion into the Cr–H bond), which causes opening of the ring, followed by insertion into one of the two formed linear chains; and (c)  $\beta$ -hydride transfer involving a second Cr site located at suitable distance. In this regard, it is worth mentioning that FTIR spectroscopy reveals, even at relatively short polymerization times, an agostic interaction between the CH<sub>2</sub> groups of a growing polymeric chain and Cr centers [5,13]. Finally, an agostically assisted mechanism has been claimed for the propagation step in ethylene polymerization on an alkyl-Cr(IV) silica-supported system that reproduces the activity of the Phillips catalyst [56,57].

### 3.4. Effect of strong ligands (NO, O<sub>2</sub>) on the “anomalous” bands

To reinforce and confirm the origin of the anomalous bands and their assignment, and thus to fully identify the initiation steps of the polymerization reaction, we proceeded in the direction documented for CO. In particular, we attempted to interfere with the polymerization mechanism shown in Scheme 1b by contacting the reacting sample (i.e., in the presence of C<sub>2</sub>H<sub>4</sub>) with stronger poisons, such as NO and O<sub>2</sub>. The dosage of these gases into the reaction cell, at a reaction step corresponding to the gray curve in Fig. 1b, immediately stopped the polymerization reaction. The results are shown in Figs. 3 and 4. Admission of 30 Torr of NO into the cell (the dotted curves

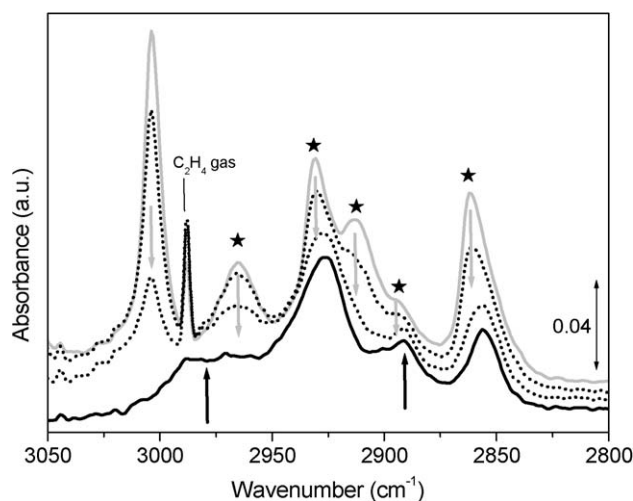


Fig. 3. Evolution of the anomalous bands upon NO dosage. Symbols as in Fig. 1. Gray spectrum: anomalous bands obtained in the same conditions of that reported in Fig. 1b. Dotted spectra: effect of NO dosage, successive contact times. Black spectrum: effect of successive outgassing at RT. Gray and black arrows show the decrease of the anomalous bands and the growth of the new components upon NO addition, respectively.

in Fig. 3) led to the following: (a) immediate disappearance of the anomalous bands (see the gray arrows), (b) disappearance of the bands of the Cr(II)···(C<sub>2</sub>H<sub>4</sub>)<sub>n</sub> complexes (see the gray arrow at 3004 cm<sup>-1</sup>), and (c) increment of the narrow band at 2988 cm<sup>-1</sup> due to gaseous C<sub>2</sub>H<sub>4</sub>. Meanwhile, in the NO stretching region, intense absorptions appeared in the 1900–1650 cm<sup>-1</sup> region, associated with the formation of nitrosylic species (spectral region not shown for brevity) [6,11,21]. We can explain these features by considering that NO is a stronger ligand than C<sub>2</sub>H<sub>4</sub> and thus easily displaces the C<sub>2</sub>H<sub>4</sub> molecules from the Cr(II)···(C<sub>2</sub>H<sub>4</sub>)<sub>n</sub> complexes, which could also

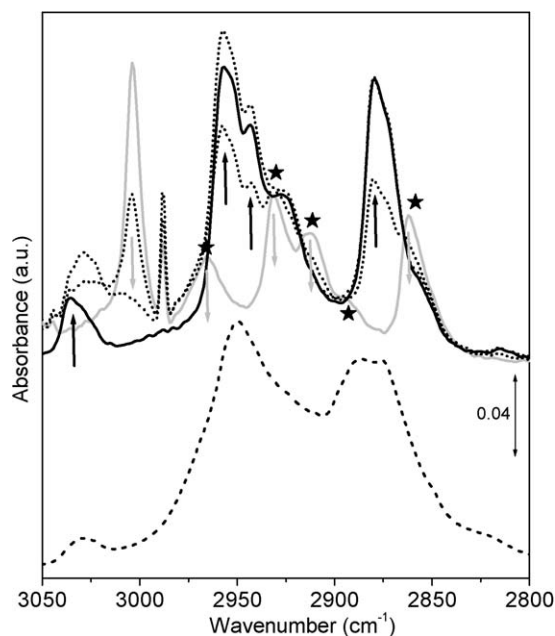
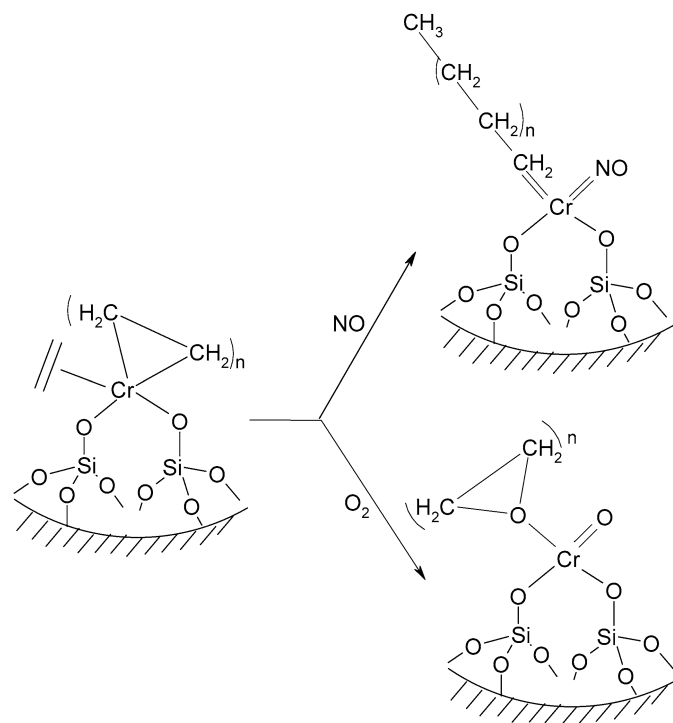


Fig. 4. Evolution of the anomalous bands upon  $O_2$  dosage. Gray spectrum: anomalous bands obtained in the same conditions of that reported in Fig. 1b. Dotted spectra: effect of  $O_2$  dosage, successive contact times. Black spectrum: effect of outgassing. The dashed spectrum reported at the bottom of the figure is obtained upon ethylene oxide interaction with Cr(II)/SiO<sub>2</sub> sample. The analogies with the black spectrum are well evident. Grey and black arrows show the decrease of the anomalous bands and the growth of the new components upon  $O_2$  addition, respectively.

be detected in the gas phase (peak at  $2988\text{ cm}^{-1}$ ) with formation of Cr(II)···(NO)<sub>2</sub> species. On outgassing the reaction cell at room temperature (bold black spectrum in Fig. 3), the resulting spectrum in the CH stretching region was characterized by two weak bands at  $2925$  and  $2855\text{ cm}^{-1}$ , which can be readily assigned to the vibrational manifestations of the few long polymeric chains grown on the Cr/SiO<sub>2</sub> sample. Together with these normal bands, a complex absorption in the  $3000$ – $2950\text{ cm}^{-1}$  range and a band at about  $2891\text{ cm}^{-1}$ , not present during the polymerization reaction, appeared (see the black arrows in Fig. 3). These bands are due to the reaction products of some of the relevant species of the “black box” with NO.

Similar behavior was observed when the polymerization was stopped by dosing  $O_2$  into the reaction cell (Fig. 4). Also in this case we observed a sudden disappearance of the anomalous bands (see the gray arrows), accompanied by the appearance of more intense and complex absorptions centred at about  $2950$  and  $2880\text{ cm}^{-1}$  and a weak band at about  $3035\text{ cm}^{-1}$  (see the black arrows). In this case the sample was completely oxidized, as demonstrated by the change in color from the blue typical of Cr(II) species to the orange of the Cr(VI) ones.

These experiments clearly demonstrate that both NO and  $O_2$  stopped the polymerization reaction immediately and, more important, significantly modified the species present during the first steps of the polymerization reaction (i.e., in the black box of Scheme 2). In particular, the anomalous bands were completely destroyed and new, different components appeared in the stretching region of the C–H modes. These observations confirm the assignment of the anomalous bands to some inter-



Scheme 4. Proposed reaction pathway followed by the intermediate metallacycle species upon interaction with NO and  $O_2$ .

mediate species that have a transient character and are stable only in the presence of sufficiently high  $C_2H_4$  pressure. These intermediate species rapidly react with NO and  $O_2$ , giving rise to various species characterized by differing vibrational features in the CH stretching region.

### 3.5. Confirmation of the initiation mechanism

The assignment of the anomalous bands advanced in Section 3.3 is strongly supported by the results concerning the reaction of the intermediate species with NO and  $O_2$  (Figs. 3 and 4, respectively). These ligands, being stronger than CO and  $C_2H_4$ , interfered not only with the propagation mechanism stopping the polymerization reaction, but also with the species contained in the black box. The Cr(II)···( $C_2H_4$ )<sub>n</sub> complexes [structure (ii) in Scheme 1b] were completely destroyed, and the species containing P<sub>1</sub> [structure (iii) in Scheme 1b] rapidly reacted, giving rise to new products characterized by differing vibrational features.

Starting with the NO case, the two stable absorptions in the  $3000$ – $2950\text{ cm}^{-1}$  region and at  $2891\text{ cm}^{-1}$  appearing after admission of NO (the bold black spectrum in Fig. 3) may be assigned to  $\nu(CH_3)$  modes of a new species derived from the opening of the small Cr-cycle intermediates. A possible reaction pathway is proposed in the top part of Scheme 4. The opening of the metallacycle species implies the formation of a  $CH_3$  group, whose asymmetric and symmetric stretching frequencies fall around  $2975$  and  $2870\text{ cm}^{-1}$ , as well as a carbenic CH group, whose vibrational manifestation may fall in the  $3000$ – $2950\text{ cm}^{-1}$  region, thus justifying the broad character of the band. The experiment demonstrates that, when present,



CH<sub>3</sub> groups are easily detectable and distinguishable from the CH<sub>2</sub> groups by FTIR spectroscopy. This once again confirms that the absence of stable bands related to CH<sub>3</sub> groups in the first stages of the polymerization should be ascribed to the absence of CH<sub>3</sub> groups in the intermediate species.

The reaction of the metallacycle intermediates with O<sub>2</sub> leads to completely different species. In this case, assignment of the resulting bands can be facilitated by comparing the spectrum with the spectrum obtained by dosing ethylene oxide on the Cr(II)/SiO<sub>2</sub> sample. In this latter case we observe, together with the bands associated with CH<sub>2</sub>OCH<sub>2</sub> adsorbed on the Cr(II) sites, the appearance of two complex absorptions at around 2935 and 2880 cm<sup>-1</sup>, which grow slowly over time. This phenomenon may be interpreted as a slow polymerization of ethylene oxide. On outgassing the sample after a few minutes of contact, we obtain the spectrum reported in Fig. 4 (bottom part, dotted line). The small band at around 3025 cm<sup>-1</sup> is a residual of the adsorbed ethylene oxide, whereas the absorption at lower frequencies is due entirely to the polymeric products. The spectrum is very similar to that obtained on reaction of O<sub>2</sub> with the intermediate species responsible for the anomalous bands and successive outgassing. This strongly suggests that one of the products of the O<sub>2</sub> reaction is ethylene oxide, which can be obtained on insertion of O into the Cr-cyclopropane cycle. A tentative reaction path is depicted at the bottom of Scheme 4. According to this interpretation, the two sets of complex bands centered at about 2950 and 2880 cm<sup>-1</sup> may be explained in terms of ν(CH<sub>2</sub>) modes of CH<sub>2</sub> groups perturbed by the presence of neighboring O, inserted into cycles of greater dimension.

#### 4. Conclusion

This work presents the first spectroscopic evidence, by means of in situ FTIR, of the occurrence of metallacycle intermediate species during ethylene polymerization on the Cr(II)/SiO<sub>2</sub> Phillips catalyst. This observation allows us to propose that the initiation mechanism follows a metallacycle route, thus clarifying a question that has remained open from 1950 to now. It is worth mentioning that the metallacycle mechanism has been shown to occur for several ethylene trimerization and tetramerization catalysts [47,49–51,53] and for homogeneous Cr catalysts [55]. For these systems, both the oxidative coupling of the first two ethylene molecules to form the metallacyclopentane intermediate [51,58] and the insertion of an additional ethylene into the metallacyclopentane species [59,60] have been claimed to constitute the rate-determining step. Very recently, van Rensburg et al. [54] calculated that the rate-determining step in the mechanism for the Phillips catalyst is the step involving growth of Cr-cyclopentane to Cr-cycloheptane, in perfect agreement with findings of Espelid and Børve [61,62]. Whatever the rate-determining step, the results given here lead to the conclusion that the more stable intermediates (i.e., the more easily detectable species) should be small, strained metallacycles. The evolution of the reaction toward the propagation and the absence of competitive reactions leading to the formation of 1-alkenes (as occurs for the oligomerization catalysts) can be

explained in terms of the low stability of the metallacycle intermediates and/or a cooperative effect of suitably spaced Cr–Cr couples.

#### Acknowledgments

The financial support of Ministero dell'Istruzione, dell'Università e della Ricerca (MIUR) and of Compagnia di San Paolo is acknowledged.

#### References

- [1] K.H. Theopold, *Eur. J. Inorg. Chem.* (1998) 15.
- [2] K.H. Theopold, *Chemtech* 27 (1997) 26.
- [3] P. Cossee, *J. Catal.* 3 (1964) 80.
- [4] J.P. Hogan, R.L. Banks, US Patent 2,825,721 (1958).
- [5] E. Groppo, C. Lamberti, S. Bordiga, G. Spoto, A. Zecchina, *Chem. Rev.* 105 (2005) 115.
- [6] A. Zecchina, E. Garrone, C. Morterra, S. Coluccia, *J. Phys. Chem.* 79 (1975) 978.
- [7] A. Zecchina, E. Garrone, G. Ghiotti, S. Coluccia, *J. Phys. Chem.* 79 (1975) 972.
- [8] B.M. Weckhuysen, R.A. Schoonheydt, J.M. Jehng, I.E. Wachs, S.J. Cho, R. Ryoo, S. Kijlstra, E. Poels, *J. Chem. Soc., Faraday Trans.* 91 (1995) 3245.
- [9] B.M. Weckhuysen, I.E. Wachs, R.A. Schoonheydt, *Chem. Rev.* 96 (1996) 3327.
- [10] B. Rebenstorf, R. Larsson, *Z. Anorg. Allg. Chem.* 478 (1981) 119.
- [11] G. Ghiotti, E. Garrone, G. Della Gatta, B. Fubini, E. Giamello, *J. Catal.* 80 (1983) 249.
- [12] E. Garrone, G. Ghiotti, C. Morterra, A. Zecchina, *Z. Naturforsch. B* 42 (1987) 728.
- [13] G. Ghiotti, E. Garrone, A. Zecchina, *J. Mol. Catal.* 46 (1988) 61.
- [14] B. Rebenstorf, *J. Mol. Catal.* 66 (1991) 59.
- [15] G. Ghiotti, E. Garrone, A. Zecchina, *J. Mol. Catal.* 65 (1991) 73.
- [16] E. Garrone, S. Abello, E. Borello, G. Ghiotti, A. Zecchina, *Mater. Chem. Phys.* 29 (1991) 369.
- [17] G. Spoto, S. Bordiga, E. Garrone, G. Ghiotti, A. Zecchina, G. Petrini, G. Leofanti, *J. Mol. Catal.* 74 (1992) 175.
- [18] P. Zielinski, I.G.D. Lana, *J. Catal.* 137 (1992) 368.
- [19] P.A. Zielinski, J.A. Szymura, I.G.D. Lana, *Catal. Lett.* 13 (1992) 331.
- [20] C.S. Kim, S.I. Woo, *J. Mol. Catal.* 73 (1992) 249.
- [21] A. Zecchina, G. Spoto, G. Ghiotti, E. Garrone, *J. Mol. Catal.* 86 (1994) 423.
- [22] A. Zecchina, D. Scarano, S. Bordiga, G. Spoto, C. Lamberti, *Adv. Catal.* 46 (2001) 265.
- [23] S. Bordiga, S. Bertarione, A. Damin, C. Prestipino, G. Spoto, C. Lamberti, A. Zecchina, *J. Mol. Catal. A* 204 (2003) 527.
- [24] E. Groppo, C. Lamberti, S. Bordiga, G. Spoto, A. Zecchina, *J. Phys. Chem. B* 109 (2005) 15024.
- [25] M.A. Vuurman, I.E. Wachs, D.J. Stufkens, A. Oskam, *J. Mol. Catal.* 80 (1993) 209.
- [26] T.J. Dines, S. Inglis, *Phys. Chem. Chem. Phys.* 5 (2003) 1320.
- [27] E. Groppo, A. Damin, F. Bonino, A. Zecchina, S. Bordiga, C. Lamberti, *Chem. Mater.* 17 (2005) 2019.
- [28] A. Damin, F. Bonino, S. Bordiga, E. Groppo, C. Lamberti, A. Zecchina, *ChemPhysChem* 7 (2006) 342.
- [29] E. Groppo, C. Prestipino, F. Cesano, F. Bonino, S. Bordiga, C. Lamberti, P.C. Thüne, J.W. Niemantsverdriet, A. Zecchina, *J. Catal.* 230 (2005) 98.
- [30] R. Merryfield, M.P. McDaniel, G. Parks, *J. Catal.* 77 (1982) 348.
- [31] E.M.E. van Kimmenade, A.E.T. Kuiper, Y. Tamminga, P.C. Thüne, J.W. Niemantsverdriet, *J. Catal.* 223 (2004) 134.
- [32] E. Groppo, C. Lamberti, G. Spoto, S. Bordiga, G. Magnacca, A. Zecchina, *J. Catal.* 236 (2005) 233.
- [33] M.P. McDaniel, *Adv. Catal.* 33 (1985) 47.

- [34] C. Lamberti, E. Groppo, G. Spoto, S. Bordiga, A. Zecchina, *Adv. Catal.* (2006), in press.
- [35] <http://www.novaratechnology.com/home.html>.
- [36] K. Vikulov, G. Spoto, S. Coluccia, A. Zecchina, *Catal. Lett.* 16 (1992) 117.
- [37] O.M. Bade, R. Blom, I.M. Dahl, A. Karlsson, *J. Catal.* 173 (1998) 460.
- [38] R.G. Snyder, *J. Chem. Phys.* 42 (1965) 1744.
- [39] R.G. Snyder, *J. Chem. Phys.* 47 (1967) 1316.
- [40] R.G. Snyder, S.L. Hsu, S. Krimm, *Spectrochim. Acta* 34 A (1978) 395.
- [41] R.G. Snyder, S.H. Strauss, C.A. Elliger, *J. Phys. Chem.* 86 (1982) 5145.
- [42] M.D. Porter, T.B. Bright, D.L. Allara, C.E.D. Chidsey, *J. Am. Chem. Soc.* 109 (1987) 3559.
- [43] S. Singh, J. Wegmann, K. Albert, K. Muller, *J. Phys. Chem. B* 106 (2002) 878.
- [44] S. Neumann-Singh, J. Villanueva-Garibay, K. Muller, *J. Phys. Chem. B* 108 (2004) 1906.
- [45] A. Bré, Y. Chauvin, D. Commereuc, *New J. Chem.* 10 (1986) 535.
- [46] J.X. McDermott, J.F. White, G.M. Whitesides, *J. Am. Chem. Soc.* 95 (1973) 4451.
- [47] R. Emrich, O. Heinemann, P.W. Jolly, C. Kruger, G.P.J. Verhovich, *Organometallics* 16 (1997) 1511.
- [48] N. Meijboom, C.J. Schaverien, A.G. Orpen, *Organometallics* 9 (1990) 774.
- [49] V.J. Ruddick, J.P.S. Badyal, *J. Phys. Chem. B* 102 (1998) 2991.
- [50] J.T. Dixon, M.J. Green, F.M. Hess, D.H. Morgan, *J. Organomet. Chem.* 689 (2004) 3641.
- [51] M.J. Overett, K. Blann, A. Bollmann, J.T. Dixon, D. Haasbroek, E. Killian, H. Maumela, D.S. McGuinness, D.H. Morgan, *J. Am. Chem. Soc.* 127 (2005) 10723.
- [52] A. Bollmann, K. Blann, J.T. Dixon, F.M. Hess, E. Killian, H. Maumela, D.S. McGuinness, D.H. Morgan, A. Neveling, S. Otto, M. Overett, A.M.Z. Slawin, P. Wasserscheid, S. Kuhlmann, *J. Am. Chem. Soc.* 126 (2004) 14712.
- [53] T. Agapie, S.J. Schofer, J.A. Labinger, J.E. Bercaw, *J. Am. Chem. Soc.* 126 (2004) 1304.
- [54] W.J. van Rensburg, C. Grove, J.P. Steynberg, K.B. Stark, J.J. Huysen, P.J. Steynberg, *Organometallics* 23 (2004) 1207.
- [55] A.K. Tomov, J.J. Chirinos, D.J. Jones, R.J. Long, V.C. Gibson, *J. Am. Chem. Soc.* 127 (2005) 10166.
- [56] S.L. Scott, J. Amor Nait Ajjou, *Chem. Eng. Sci.* 56 (2001) 4155.
- [57] J. Amor Nait Ajjou, S.L. Scott, *J. Am. Chem. Soc.* 122 (2000) 8968.
- [58] Y. Yang, H. Kim, J. Lee, H. Paik, H.G. Jang, *Appl. Catal. A: Gen.* 193 (2000) 29.
- [59] R.D. Kohn, M. Haufe, S. Mihan, D. Lilge, *Chem. Commun.* (2000) 1927.
- [60] P.J.W. Deckers, B. Hessen, J.H. Teuben, *Angew. Chem. Int. Ed.* 40 (2001) 2516.
- [61] O. Espelid, K.J. Borge, *J. Catal.* 195 (2000) 125.
- [62] O. Espelid, K.J. Borge, *J. Catal.* 205 (2002) 366.